Random Close Packing as a Dynamical Phase Transition

Sam Wilken, 1,* Rodrigo E. Guerra, 1 Dov Levine, 2 and Paul M. Chaikin ¹Physics Department, New York University, 726 Broadway, New York, New York 10003, USA ²Department of Physics, Technion, IIT, 32000 Haifa, Israel



(Received 4 December 2020; revised 31 March 2021; accepted 23 April 2021; published 12 July 2021)

Sphere packing is an ancient problem. The densest packing is known to be a face-centered cubic (FCC) crystal, with space-filling fraction $\phi_{FCC} = \pi/\sqrt{18} \approx 0.74$. The densest "random packing," random close packing (RCP), is yet ill defined, although many experiments and simulations agree on a value $\phi_{RCP} \approx 0.64$. We introduce a simple absorbing-state model, biased random organization (BRO), which exhibits a Manna class dynamical phase transition between absorbing and active states that has as its densest critical point $\phi_{c_{max}} \approx 0.64 \approx \phi_{RCP}$ and, like other Manna class models, is hyperuniform at criticality. The configurations we obtain from BRO appear to be structurally identical to RCP configurations from other protocols. This leads us to conjecture that the highest-density absorbing state for an isotropic biased random organization model produces an ensemble of configurations that characterizes the state conventionally known as RCP.

DOI: 10.1103/PhysRevLett.127.038002

Equal-sized spheres poured into a container can form many stable and metastable configurations that fill the volume to solid volume fractions ranging from ~0.55 to ~ 0.74 depending on friction and the protocol used [1,2]. The fact that many different experimental [3–5] and simulation [6–8] protocols with frictionless spheres tend to give a maximum packing fraction of $\phi \approx 0.64$ suggests a special state that Bernal [4] referred to as "random close packing" (RCP). There have been many attempts [9–17] to define this state mathematically, statistically, and physically. RCP is important fundamentally and practically in problems ranging from the number of gumballs in a jar to the viscosity of suspensions [18] and the rigidity of amorphous, jammed [19], and glassy [20,21] materials. In this Letter, we propose that the densest critical state in the conserved directed percolation (Manna) universality class BRO model has many of the properties previously associated with RCP, which has ramifications for the long-range structural organization of RCP.

Our path to this problem began with a beautiful experiment on the time reversibility of low-Reynolds-number flow that found that below a volume-fraction-dependent threshold cyclic shear strain, $\gamma_c(\phi)$, particles in a highly viscous fluid would return to the same position every cycle following reversible trajectories [22]. Above $\gamma_c(\phi)$, their behavior is diffusive and chaotic. A simple toy model, random organization (RO), captures the essential features of this transition [23]. In RO, phantom particles are said to be active if they overlap another particle under cyclic affine shear. After each cycle, particles are returned to their beginning position, and active particles are given a random uncorrelated displacement with typical magnitude ϵ . Particle configurations either evolve with time to an absorbing state, where no particles overlap, or they settle into a continuously evolving steady state with a finite fraction of active particles. Organization proceeds by a competition between generally lower-density quiescent regions being infected by generally higher-density active regions and active regions dying out. The characteristic time, $\tau \sim |\gamma - \gamma_c(\phi)|^{-\nu_{\parallel}}$, to organize into an absorbing state or a dynamical steady state diverges as the threshold strain is approached from above or below $\gamma_c(\phi)$, indicating a second-order dynamic phase transition. Similarly, $\tau \sim |\phi|$ $\phi_c(\gamma)|^{-\nu_{\parallel}}$ for fixed γ . The model is similar to early epidemic models such as directed percolation and is in the same universality class as the discrete Manna model [24,25].

Unlike conventional thermodynamic phase transitions, which exhibit diverging density or order parameter fluctuations at their critical point [24], the critical states of these dynamical absorbing state models have vanishing longrange density fluctuations at critical [26-28]—they are hyperuniform [29-31]. Recently, we demonstrated this hyperuniformity experimentally [32]. However, the experimental ϕ_c 's were considerably higher than those predicted by RO. We, and several previous authors, modified RO with repulsive displacements in studies of jamming [15,17] and hyperuniformity [33]. Biasing the displacements of overlapping particles away from each other shifted the critical density upward [32,34].

BRO, an absorbing-state model, remains in the Manna universality class [24] and exhibits hyperuniformity at critical with the structure factor $S(q \to 0) \sim q^{\alpha}$. For all Manna class models, $\alpha_{3D} = 0.25$ [26]. To characterize these critical configurations, we show that BRO and two other jamming protocols for RCP have very similar S(q)'s, with the hyperuniformity scaling exponent $\alpha \sim 0.25$. We

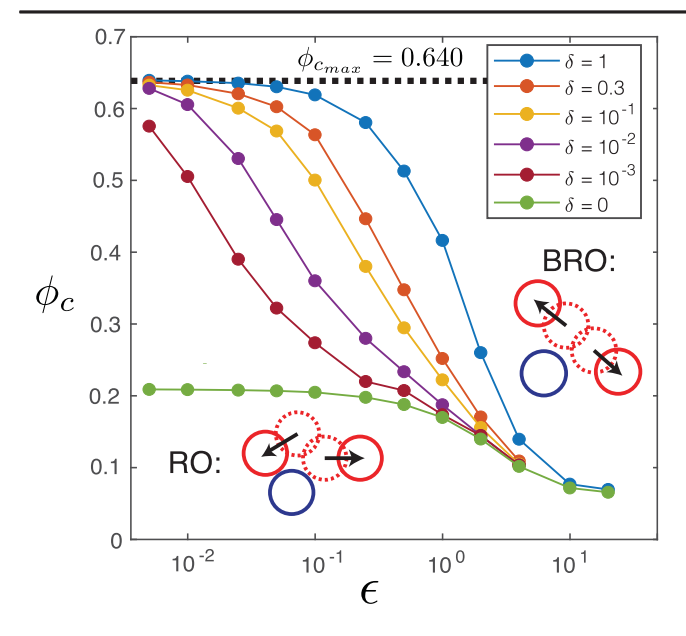


FIG. 1. The critical volume fraction ϕ_c for 3D biased random organization (BRO) as a function of the displacement magnitude ϵ . Traces correspond to different ratios of variance of repulsive to random displacements δ , where $\delta=1$ (blue) consists of purely repulsive displacements, whereas $\delta=0$ (green) is random organization (RO) with all random displacements. For $\delta>0$, the small- ϵ limit for any fixed ratio of repulsive displacements $\phi_c(\epsilon\to0)\approx 0.640\pm0.001\approx \phi_{RCP}$.

also find isostatic coordination Z=6, and a similar radial distribution function as found in several previous RCP experiments [4,35–37] and simulations [8,33,38], giving us confidence to conclude that the critical states of BRO are RCP configurations. RCP's identification as a dynamical phase transition critical point may provide new insights into disorder, jamming, and glass transitions. BRO at the

maximum-density critical point seems to produce the same ensembles as previous protocols.

In the BRO model, active (overlapping) particles are given two displacements: a repulsive displacement of magnitude $\sqrt{\delta}\epsilon$, away from the center of the overlapping cluster, and a randomly directed displacement of magnitude $\sqrt{1-\delta}\epsilon$, where for a given simulation δ is fixed at a value between 0 and 1 while displacement magnitudes are randomly distributed between 0 and $\epsilon d/2$, for particle diameter d, which determines the volume fraction, ϕ . Thus, the BRO model has two control parameters, δ and ϵ (See the Supplemental Material [39]). Hereafter, we only consider isotropic unsheared dynamics: $\gamma=0$.

The addition of repulsive bias to the particle displacements vastly changes ϕ_c in the region where ϵ is small, as shown in Fig. 1. In the $\epsilon \to 0$ limit, ϕ_c increases well above the unbiased RO limit, $\phi_c(\epsilon \to 0, \delta = 0) = \phi_{c_{\max}}(\delta = 0) \approx 0.20$, and it plateaus at $\phi_c(\epsilon \to 0, \delta > 0) = \phi_{c_{\max}}(\delta > 0) = 0.640 \approx \phi_{RCP}$. This is the case not only for $\delta = 1$, but for any $\delta > 0$. For all δ and $\epsilon \gg$ particle separations, displacements are effectively random, and hence are mean field, and we find $\phi_c(\epsilon \to \infty, 0 \le \delta \le 1) \to 0.06$. ϕ_c errors are roughly constant: 0.001 for each point.

To test whether BRO remains in the Manna universality class, we measure the critical exponents for the steady-state activity f_a^∞ and the relaxation times τ from a random initial state for $\delta=1$. Steady-state values of f_a^∞ for BRO with decreasing values of ϵ , for the RO model with $\epsilon=1$ and for the Manna model, collapse when rescaling f_a^∞ by $A/\sqrt{\epsilon}$ and rescaling $(\phi-\phi_c)/\phi_c$ by $\phi^{-1/\beta}$, where β is the activity exponent, as shown in Fig. 2(a). A is a fitted scaling parameter that is 1 for the RO and BRO models and 20 for the Manna model. A reflects the difference in how excluded volume is implemented in different models. For all models,

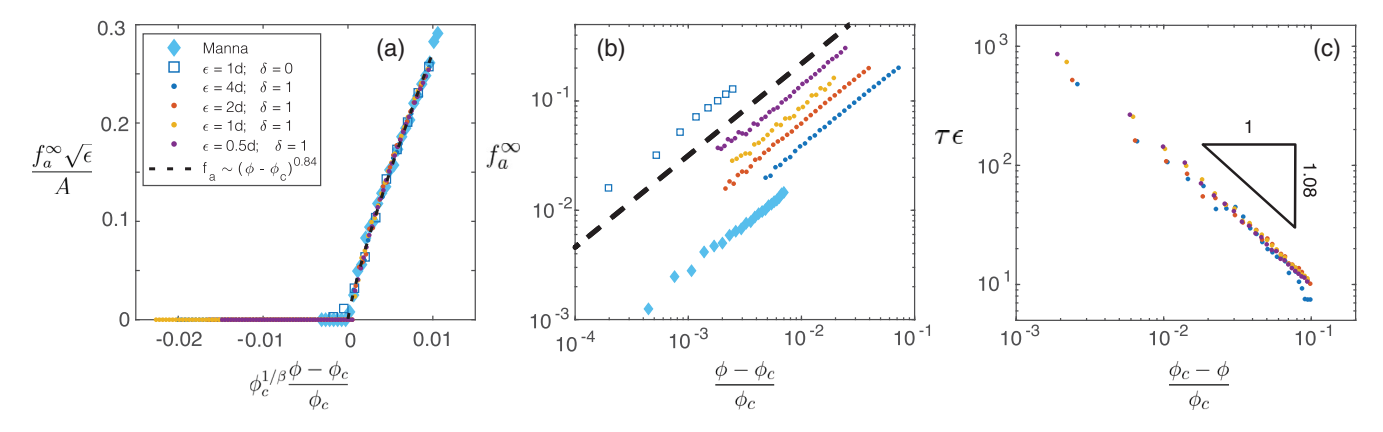


FIG. 2. Manna universal scaling of biased random organization. (a) The steady-state activity f_a^∞ is plotted as a function of the reduced control parameter $(\phi - \phi_c)/\phi_c$, showing a clear transition between absorbing $f_a^\infty = 0$ and active $f_a^\infty > 0$ states. The data for decreasing ϵ values of the BRO model are collapsed with the RO model $\delta = 0$ (blue squares) and the Manna model (light blue diamonds). Collapse requires rescaling the reduced control parameter by $\phi_c^{(-1/\beta)}$ and rescaling the activity by $A/\sqrt{\epsilon}$. (b) The same data from (a) are displayed using log-log plotting to show power-law scaling of f_a^∞ above the critical point. All models show Manna/RO class scaling $f_a^\infty \sim (\phi - \phi_c)^\beta$, where $\beta = 0.84$ in 3D. (c) For $\delta = 1$ and epsilon corresponding to parts (a) and (b), the characteristic relaxation times τ from a Poisson random initial state to an absorbing state are plotted to show power-law divergence at ϕ_c .

 f_a^{∞} vanishes at ϕ_c with $f_a^{\infty} \sim (\phi - \phi_c)^{\beta}$, where β is a Manna critical exponent, $\beta = 0.84$ in 3D, as shown in Fig. 2(b).

Similarly, we investigate the relaxation time τ by fitting the evolution of the activity to a form [23] $f_a(t) = (f_a(0) - f_a(\infty))e^{-t/\tau}(t/t_0)^{-\xi} + f_a(\infty)$, where $\xi = 0.7 \pm 0.1$ for all simulations in 3D. Relaxation times for BRO scale as $\tau \sim |\phi - \phi_c|^{-\nu_{\parallel}}$ on both the absorbing and active sides of the transition with the same $\nu_{\parallel} = 1.08$ exponent characteristic of the 3D Manna transition. Rescaling the relaxation times by $1/\varepsilon$ on the absorbing side and plotting them as functions of $(\phi - \phi_c)/\phi_c$ collapses the data, as shown in Fig. 2(c).

In addition to a characteristic volume fraction ϕ_{RCP} , sphere-packing experiments [4,35–37] and simulations [8,33,38] find universal structural features that characterize RCP states. Correspondence between the BRO critical point and previous studies of RCP requires that structures found by BRO match those found by previous methods; we choose the Lubachevsky-Stillinger (LS) [48] and soft sphere algorithms [8] as benchmark models.

The pair correlation function g(r) measures the isotropic real-space pairwise particle correlations in the system. For BRO with decreasing values of ϵ and $\delta=1$, all critically organized structures exhibit an excluded volume region of 0 < r < d (inactive particles do not overlap). The first peak of g(r) corresponds to the distance of nearest neighbors and becomes taller and sharper as $\epsilon \to 0$, as shown in Fig. 3(a). We also observe a split in the second-nearest neighbor peak for small ϵ values with cusps at $r = \sqrt{3}d$ and r = 2d, which is a signature of RCP structures [33,35] [Fig. 3(a), inset].

In RCP systems, short-range particle correlations are characterized by two features: a delta function at |r| = dfollowed by a power-law decay [49] $g(r) \sim (r/d-1)^{-1/2}$ as $r \to d^+$. For critical BRO configurations, power-law scaling of g(r) is evident, but only over an appreciable range as $\epsilon \to 0$ [Fig. 3(b)]. In this limit, it is also evident that the nearest neighbor peak narrows, it becomes taller, and the position of its maximum shifts towards r = d, consistent with delta-function scaling as $\epsilon \to 0$ (in Fig. 3 (a)). The integral of this peak is associated with another property of RCP and Jamming: the average number of particles in contact with a reference particle, Z. In BRO, particles are given finite repulsive displacements, so inactive particles are never precisely in contact, but they will touch as $\epsilon \to 0$. As in previous studies [33], we count the particles whose surfaces are within a cutoff distance x_{cut} , defining $Z(x_{\text{cut}}) = (24\phi_c)/d^3 \int_d^{d+x_{\text{cut}}} g(r) r^2 dr$. For critical BRO, Z rises as $x_{\rm cut}$ increases, plateauing close to $x_{\rm cut} \approx$ $\epsilon/2$ and rising again after. The second rise in Z is largely independent of ϵ , making the plateau flatter and more obvious as $\epsilon \to 0$. Fitting the plateau regions to a power law with a constant offset, we find that the plateau of Z approaches 6, matching the isostatic condition expected for frictionless spheres [Fig. 3(c)]. Many other RCP and jamming experiments [4] and simulations [8,17,33], even those with inherent polymeric connectivity [50], find $Z \approx 6$, and the power law that we find is similar to the near-contact Z calculated in the LS model [33]. The isostatic coordination has implications for the mechanical properties of the packings—for example, the vanishing of the shear modulus at RCP, the source of which is nonaffine particle displacements [8,51]. We leave further investigation to future work.

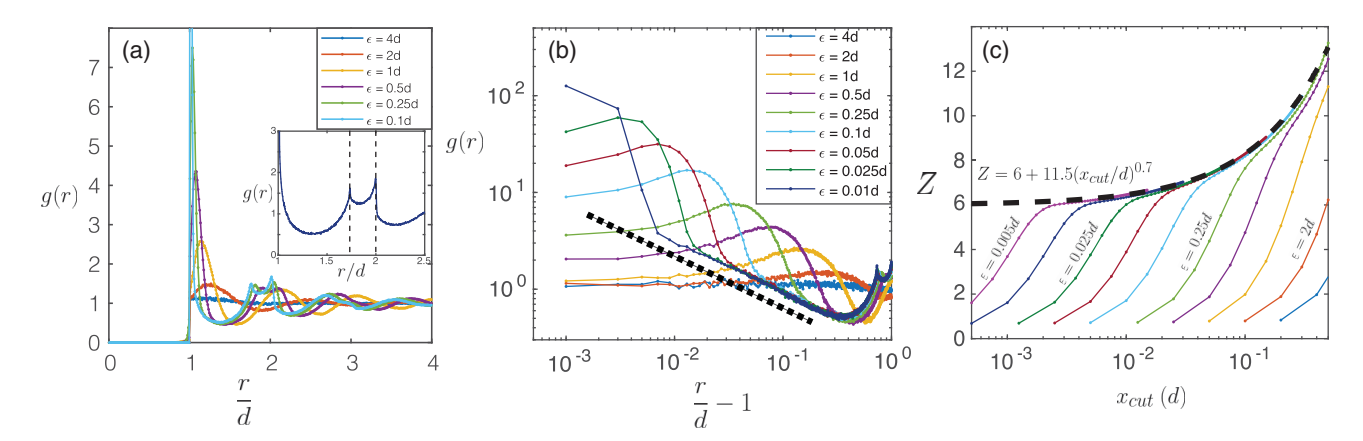


FIG. 3. Random close packing structure at $\phi_c(\epsilon \to 0)$ for $\delta = 1$. (a) The pair correlation function g(r) is plotted for critical structures of BRO. All show an expected excluded volume region which corresponds to the particle size and a strong diverging peak at the nearest neighbor separation in the $\epsilon \to 0$ limit. *Inset*: The split in the second-nearest neighbor peak occurs at small epsilon ($\epsilon = 0.025d$ is shown). The cusps at $r = \sqrt{3}d$ and r = 2d (–) are consistent with previous RCP studies. (b) A log-log plot of g(r) at ϕ_c as a function of r/d-1 emphasizes the power-law decay of g(r) away from r=d. Small- ϵ structures at ϕ_c show $g(r) \sim (r/d-1)^{-0.5}$ (––). (c) The average contact number Z is counted for critical structures where Z is the number of neighbors at a distance less than $d+x_{\rm cut}$ from a target particle. For each structure, Z is undercounted if $x_{\rm cut}$ is too small, but as $\epsilon \to 0$, Z approaches a plateau at the isostatic limit Z=6. The overcounted structures fit a form close to previous RCP calculations [33].

Thinking of critically organized structures within the framework of hyperuniformity [29] emphasizes the role of long-range density correlations. There have been a few studies of long-range correlations in RCP systems, but with controversial results and significant disagreements between experiments [52] and simulations [30]. We investigate the hyperuniformity of BRO by looking for power-law scaling of $S(q \to 0) \sim q^{\alpha}$. We calculate S(q) for fully relaxed $(t \gg \tau)$ simulations at ϕ_c for various values of ϵ and $\delta = 1$. We find hyperuniform scaling $S(q \to 0) \sim q^{\alpha}$ with $\alpha \approx$ 0.25 for all critical structures, even those with critical volume fractions approaching $\phi_c \rightarrow \phi_{RCP}$ [Fig. 4(a)]. $\alpha =$ 0.25 is the critical exponent for 3D Manna class systems [26], and it is the same exponent found recently in experiments on critically sheared colloids [32]. The robustness of this hyperuniform scaling exponent provides more evidence that BRO is in the Manna universality class.

Previous studies of RCP structures using Lubachevsky-Stillinger algorithm identified hyperuniform scaling near the maximally random jammed (MRJ) point [9,30]; however, from a linear plot, they concluded $S(q \to 0) \sim q^{1}$. We reproduce those data here, and we include results from our own simulations of the soft sphere model relaxed by conjugate gradient energy minimization [8,39]. Although there is a region $q \sim 0.08-0.5$ that can be fit with a power $\alpha \approx 1$, over the lower q region $q \approx$ 0.006–0.08, we find $\alpha_{LS} = 0.24 \pm 0.02$. The three RCP models display very similar S(q)'s for all values of q. While there is surprising agreement in S(q) at ϕ_{RCP} , this is not the case away from ϕ_{RCP} . A measure of the difference is $\Delta S(q) = \int_0^{5(2\pi/d)} |S(q,\phi)/S(q,\phi_c) - 1| dq$. At ϕ_c , all models have approximately the same $\Delta S(q)$. However, the inset of Fig. 4(b) shows significant differences between the models on both sides of the transition, which implies that BRO is not a disguised form of a previously studied model. It is remarkable that several different protocols converge to RCP but approach it differently as a function of ϕ .

There have been many previous protocols to find RCP. Several authors use jamming in their constructions [8,9,14,15,17,53], others use a peaked statistical ensemble of accessible states from energy minimization [11,53], and others look for randomness as a minimization of many order parameters—e.g., MRJ [9]. A different form of hyperuniformity, "contact hyperuniformity," was found for jammed packings [54]. BRO at the maximum-density critical point seemingly produces the same ensemble as many of the previous protocols. We note that regarding RCP as the highest-density critical point of a dynamic phase transition requires invoking neither randomness, nor jamming, nor hyperuniformity in the outcome; rather, they are emergent properties.

Unresolved is the question of why the BRO critical point is seemingly coincident at ϕ_{RCP} with the results of previous protocols. In some sense, the BRO critical point is similar to the soft sphere calculations, in that there are directed

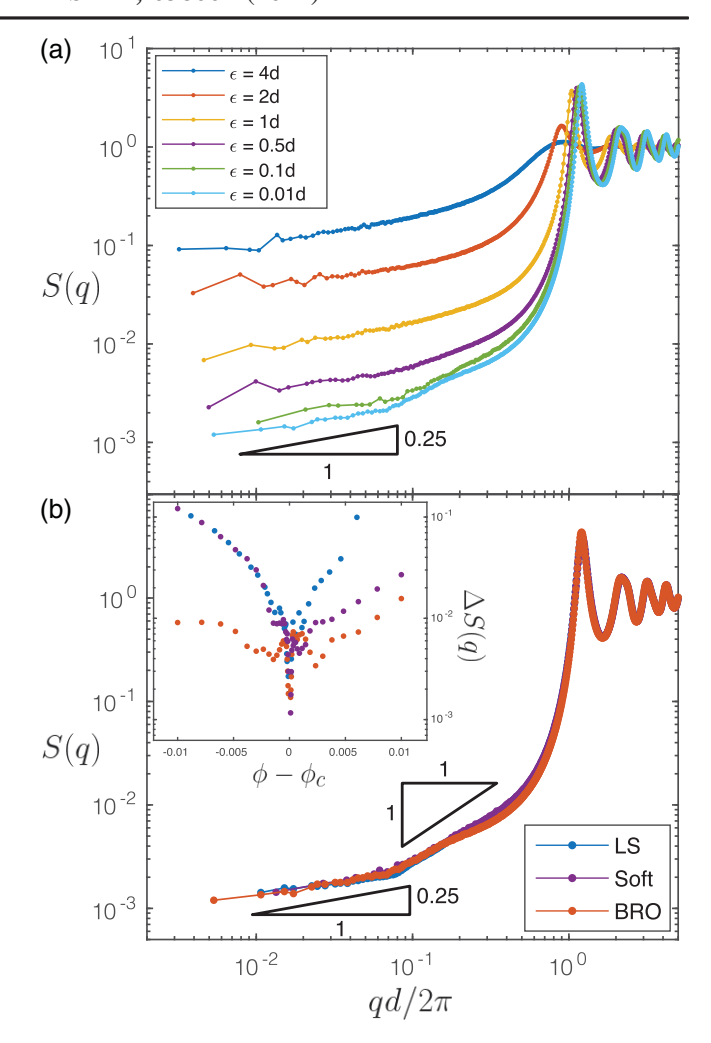


FIG. 4. Random close packing is Manna class hyperuniform. (a) The angularly averaged structure factor S(q) is plotted for BRO structures at ϕ_c . Different traces correspond to decreasing ϵ values where all critical structures are hyperuniform with Manna universal scaling $S(q \to 0) \sim q^{0.25 \pm 0.01}$ for all ϵ values. (b) The critical structure factor S(q) for three models of RCP: Lubachevsky-Stillinger (data from Donev et~al.) [30], soft spheres, and BRO. The structure factors calculated from LS and soft spheres agree remarkably well with the $\epsilon \to 0$ limit of BRO, all three showing $S(q \to 0) \sim q^{\alpha}$. Manna class hyperuniform scaling is according to $\alpha_{LS} = 0.24 \pm 0.02$, $\alpha_{Soft} = 0.27 \pm 0.03$, and $\alpha_{BRO} = 0.26 \pm 0.02$. Inset: The relative difference structure factor $\Delta S(q) = \int_0^{5(2\pi/d)} |S(q,\phi)/S(q,\phi_c) - 1|dq$ is a measure of S(q) away from ϕ_c . Though all models agree at the critical point $\Delta S \approx 0$, they differ on both sides of the transition.

repulsive steps in both. Soft spheres equilibrate more slowly as RCP is approached from both sides. Our preliminary investigation suggests that the soft sphere model may also be related to a dynamical phase transition, as also suggested in Ref. [17].

BRO can be investigated in other dimensions. In 1D, the densest monodispersed absorbing state has $\phi_c = 1$ and is trivially a 1D crystal (while for RO $\phi_c \approx 0.9$). In 2D, we

find that the densest monodispersed BRO absorbing state approaches a densely packed hexagonal crystal with $\phi_c \approx 0.91$, (while for RO $\phi_c \approx 0.45$). With bi-dispersed disks, the results are similar to jammed states found in the literature, but we also find $S(q) \sim q^{\alpha}$ with $\alpha \approx 0.45$, which is the 2D Manna hyperuniformity exponent (see the Supplemental Material [39]), lending credence to our claim that RCP in 3D is indeed hyperuniform with Manna class exponents. We have not yet studied BRO in greater than 3D. In 3D, BRO yields FCC crystals when sheared, hence the "isotropic" in our conjecture.

Biased random organization is a well-defined dynamical model and protocol, especially in the $\epsilon \to 0$ limit. We have demonstrated that in the thermodynamic limit (infinite size system) for vanishingly small displacements ($\epsilon \to 0$), the highest-density absorbing state has many properties coincident with those associated with RCP or "point J" in the jamming phase diagram. With this association of RCP with the critical point of a dynamic phase transition, we expect progress in mathematically calculating ϕ_{RCP} , gaining insight into the properties of the jamming and glass transitions and studies of amorphous systems in general.

This work was supported primarily by the MRSEC Program of the National Science Foundation under Grant No. DMR-1420073 (S. W.) for simulations; partially supported by the Center for Bio-Inspired Energy Sciences (CBES), an Energy Frontier Research Center funded by the U.S. DOE, Office of Sciences, Basic Energy Sciences under Award No. de-sc0000989 (R. E. G., P. M. C.) for calculations; and supported by the National Science Foundation Physics of Living **Systems** Grant No. 1504867(P. M. C., D. L.), NASA under Grant No. NNX13AR67G (REG), and NSF CBET 1832260: GOALI (P. M. C.) for theory. D. L. also acknowledges the support of the US-Israel Binational Science Foundation (Grant No. 2014713) and the Israel Science Foundation (Grant No. 1866/16). We are particularly thankful to Professor Aleks Donev for useful discussions and for providing the dataset from Ref. [30] for use in Fig. 4(b) to compare hyperuniformity exponents. We thank Professors David Pine, Daniel Hexner, Sal Torquato, and Stefano Martiniani for useful discussions. We thank Yael Strulovitch for the Editors' Suggestion image.

Note added in the proof.—After the acceptance of our work, we became aware of [55] for the Rissone paper.

- *srw346@nyu.edu
- [1] P. Ball, Nature (London) 480, 455 (2011).
- [2] T. C. Hales, Ann. Math. 162, 1065 (2005).
- [3] G. D. Scott, Nature (London) 188, 908 (1960).
- [4] J. D. Bernal and J. Mason, Nature (London) 188, 910 (1960).

- [5] E. R. Nowak, J. B. Knight, E. Ben-Naim, H. M. Jaeger, and S. R. Nagel, Phys. Rev. E 57, 1971 (1998).
- [6] A. Z. Zinchenko, J. Comput. Phys. 114, 298 (1994).
- [7] B. D. Lubachevsky, F. H. Stillinger, and E. N. Pinson, J. Stat. Phys. 64, 501 (1991).
- [8] C. S. O'Hern, L. E. Silbert, A. J. Liu, and S. R. Nagel, Phys. Rev. E 68, 011306 (2003).
- [9] S. Torquato, T. M. Truskett, and P. G. Debenedetti, Phys. Rev. Lett. 84, 2064 (2000).
- [10] R. D. Kamien and A. J. Liu, Phys. Rev. Lett. **99**, 155501
- [11] P. Charbonneau, E. I. Corwin, G. Parisi, and F. Zamponi, Phys. Rev. Lett. 109, 205501 (2012).
- [12] J. G. Berryman, Phys. Rev. A 27, 1053 (1983).
- [13] C. Song, P. Wang, and H. A. Makse, Nature (London) 453, 629 (2008).
- [14] M. Wyart, Phys. Rev. Lett. 109, 125502 (2012).
- [15] C. Ness and M. E. Cates, Phys. Rev. Lett. 124, 088004 (2020).
- [16] F. Krzakala and J. Kurchan, Phys. Rev. E 76, 021122 (2007).
- [17] L. Milz and M. Schmiedeberg, Phys. Rev. E 88, 062308 (2013).
- [18] M. Wyart and M. E. Cates, Phys. Rev. Lett. **112**, 098302 (2014).
- [19] A. J. Liu and S. R. Nagel, Nature (London) **396**, 21 (1998).
- [20] J. D. Bernal, Nature (London) 183, 141 (1959).
- [21] P. N. Pusey and W. van Megen, Phys. Rev. Lett. 59, 2083 (1987).
- [22] D. J. Pine, J. P. Gollub, J. F. Brady, and A. M. Leshansky, Nature (London) 438, 997 (2005).
- [23] L. Corté, P. M. Chaikin, J. P. Gollub, and D. J. Pine, Nat. Phys. 4, 420 (2008).
- [24] M. Henkel, H. Hinrichsen, S. Lübeck, and M. Pleimling, Non-Equilibrium Phase Transitions, Theoretical and Mathematical Physics (Springer, Dordrecht, Netherlands; New York, 2008).
- [25] G. I. Menon and S. Ramaswamy, Phys. Rev. E **79**, 061108 (2009).
- [26] D. Hexner and D. Levine, Phys. Rev. Lett. **114**, 110602 (2015).
- [27] K. J. Schrenk and D. Frenkel, J. Chem. Phys. 143, 241103 (2015).
- [28] E. Tjhung and L. Berthier, Phys. Rev. Lett. **114**, 148301 (2015).
- [29] S. Torquato and F. H. Stillinger, Phys. Rev. E **68**, 041113 (2003).
- [30] A. Donev, F. H. Stillinger, and S. Torquato, Phys. Rev. Lett. **95**, 090604 (2005).
- [31] S. Torquato, Phys. Rep. Hyperuniform State Matter **745**, 1 (2018).
- [32] S. Wilken, R. E. Guerra, D. J. Pine, and P. M. Chaikin, Phys. Rev. Lett. **125**, 148001 (2020).
- [33] A. Donev, S. Torquato, and F. H. Stillinger, Phys. Rev. E **71**, 011105 (2005).
- [34] D. Hexner and D. Levine, Phys. Rev. Lett. 118, 020601 (2017).
- [35] G. D. Scott, Nature (London) 194, 956 (1962).
- [36] J. L. Finney and J. D. Bernal, Proc. R. Soc. A. 319, 479 (1970).

- [37] T. Aste, M. Saadatfar, and T. J. Senden, Phys. Rev. E 71, 061302 (2005).
- [38] G. Parisi and F. Zamponi, J. Chem. Phys. 123, 144501 (2005).
- [39] See Supplemental Material at http://link.aps.org/supplemental/ 10.1103/PhysRevLett.127.038002, which includes Refs. [8, 23,32,33,40–47] for additional simulation details.
- [40] M. Skoge, A. Donev, F. H. Stillinger, and S. Torquato, Phys. Rev. E 74, 041127 (2006).
- [41] A. Donev, S. Torquato, and F.H. Stillinger, J. Comput. Phys. 202, 737 (2005).
- [42] J. A. Anderson, J. Glaser, and S. C. Glotzer, Comput. Mater. Sci. **173**, 109363 (2020).
- [43] C. L. Phillips, J. A. Anderson, and S. C. Glotzer, J. Comput. Phys. 230, 7191 (2011).
- [44] E. Bitzek, P. Koskinen, F. Gähler, M. Moseler, and P. Gumbsch, Phys. Rev. Lett. 97, 170201 (2006).
- [45] S. Atkinson, F. H. Stillinger, and S. Torquato, Proc. Natl. Acad. Sci. U.S.A. 111, 18436 (2014).

- [46] C. E. Zachary, Y. Jiao, and S. Torquato, Phys. Rev. E 83, 051308 (2011).
- [47] D. Henderson, Mol. Phys. 30, 971 (1975).
- [48] B. D. Lubachevsky and F. H. Stillinger, J. Stat. Phys. **60**, 561 (1990).
- [49] L. E. Silbert, D. Ertaş, G. S. Grest, T. C. Halsey, and D. Levine, Phys. Rev. E 65, 031304 (2002).
- [50] N. C. Karayiannis, K. Foteinopoulou, and M. Laso, Phys. Rev. E 80, 011307 (2009).
- [51] A. Zaccone and E. Scossa-Romano, Phys. Rev. B 83, 184205 (2011).
- [52] R. Kurita and E. R. Weeks, Phys. Rev. E **82**, 011403 (2010).
- [53] S. Martiniani, K. J. Schrenk, K. Ramola, B. Chakraborty, and D. Frenkel, Nat. Phys. 13, 848 (2017).
- [54] D. Hexner, A. J. Liu, and S. R. Nagel, Phys. Rev. Lett. 121, 115501 (2018).
- [55] P. Rissone, E. I. Corwin, and G. Parisi, preceding Letter, Phys. Rev. Lett. 127, 038001 (2021).